Strong-axis flexural buckling of cellular and castellated members

Delphine Sonck[1], Jan Belis[2]

Abstract
Cellular and castellated members are steel I-section members with circular or hexagonal web openings placed at regular intervals along the member's length. Compared with a member without web openings, these members have a more optimal material use in strong-axis bending. Other advantages are the savings in construction height possible by guiding service ducts through the web openings and aesthetics. However, compared with unperforated members, the resistance checks will be more complex and the fabrication cost will be higher.

Depending on the boundary and loading conditions, flexural buckling about the strong axis could contribute to the failure of cellular or castellated columns or beam-columns. The corresponding critical buckling load of castellated and cellular columns is expected to be smaller than that of a similar I-section column without web openings, due to the decreased shear stiffness of the web. This is caused by the local bending and shear deformations around the openings. However, research covering this aspect is limited.

In this paper, the elastic strong-axis flexural buckling behavior of castellated and cellular members will be investigated by means of a numerical parametric study. It will be shown that the existing formulations for the critical buckling load are still unsafe. Thus, a new expression for the critical buckling load will be proposed, based on an adaptation of the approach used for flexural buckling of battened columns.

1. Introduction

Cellular and castellated members are steel I-section members with large circular or hexagonal web openings in their webs, appearing at regular intervals in length direction. Because of these web openings, their strong-axis bending resistance will be optimized: for the same amount of material, the resistance will be higher than for I-section members without web openings. Additional cost savings are possible by the ability to guide service ducts though the openings, saving construction height. A last advantage is their lighter appearance. However, the presence of the web openings will modify the failure behavior of cellular and castellated members.

Cellular and castellated members are predominantly used for beams, but they can also be used as columns. This can be out of aesthetic considerations, but also because the column is subjected to a combination of strong-axis bending and compression. Over the past years, a considerable amount of research has focused on the lateral-torsional buckling behavior of castellated and

---

[1] Post-doctoral assistant, Ghent University, <Delphine.Sonck@UGent.be>
[2] Professor, Ghent University, < Jan.Belis@UGent.be >

cellular beams (Ellobody 2011; Nethercot and Kerdal 1982; Nseir et al. 2012; Sonck 2014; Sonck and Belis 2015; Zirakian 2006). However, the existing research about flexural buckling of cellular and castellated columns is much more limited. Depending on the boundary conditions, compressed columns can fail by strong-axis flexural buckling (Fig. 1). For this buckling type, the presence of the web openings will influence the critical buckling load detrimentally, due to the decreased shear stiffness of the web caused by local deformations around the web openings.
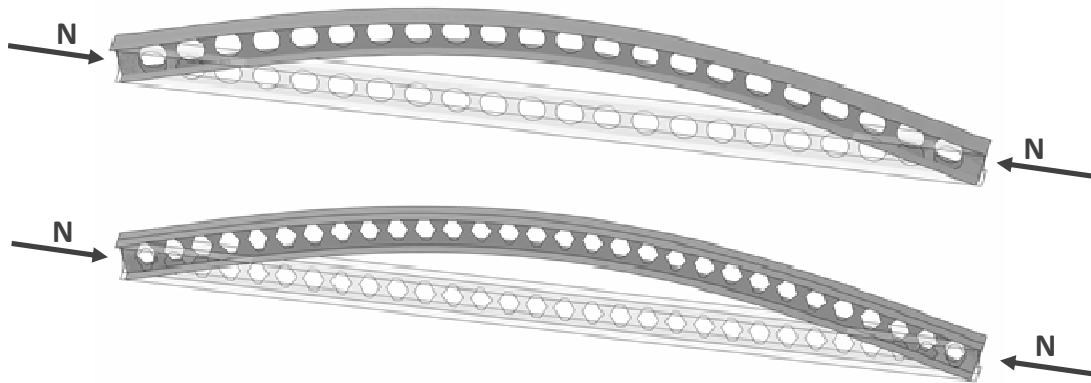

Figure 1: Strong axis flexural buckling of cellular and castellated columns.

Research about the strong-axis flexural buckling behaviour is relatively limited. All existing research focuses on the elastic critical buckling load formulation. In (Sweedan et al. 2009), the critical buckling load of cellular columns is investigated. It is proposed to use a tabulated reduction factor for the critical Euler buckling load. Additionally, the approach used for battened columns as proposed in (Timoshenko and Gere 1961) was considered. However, this was found to be overly conservative. In (El-Sawy et al. 2009), a similar investigation was executed for castellated columns, where it was proposed to use charted values for a buckling modification factor that takes into account the effect of the shear stiffness of the web. In both papers, the introduced modification factors should be determined using charts based on the numerical results, which is not very convenient. However, a more appropriate closed expression for the critical buckling load is given in (Yuan et al. 2014) for castellated columns and in (Gu and Cheng 2016) for cellular columns. More details about these closed expressions and their derivation is given in Sections 2.2 and 2.3. The amount of geometries for which these expressions was validated was limited.

In this paper, the closed expressions for the critical buckling load, given in (Yuan et al. 2014) and (Gu and Cheng 2016) will be checked in a larger numerical parametric study. Additionally, it will be investigated whether the approach used for battened columns could be modified to make it more precise. In this investigation, only simply supported, doubly symmetric castellated or cellular columns loaded by a central compressive force N will be considered.

In the next section, the already existing formulations for the strong-axis critical buckling load N_{cr} of castellated and cellular columns will be discussed. Subsequently, it will be shown how the existing approach for battened columns could be modified to obtain a new, more precise formulation of N_{cr}. All these formulations will be compared with the numerical results obtained using the numerical model and parametric study described in the next section. Finally, a detailed

2

comparison of the numerical and analytical results is described, illustrating the suitability of the new formulation.

2. Existing design rules for strong-axis flexural buckling
In this section, an overview will be given of the different existing formulations for the strong-axis critical buckling load that could be suitable for cellular and castellated members.

2.1 Critical load of built-up columns
As first derived by Engesser, the effect of the shear deformation can decrease the critical Euler buckling load N_{cr} (Eq. 1) to a critical buckling load $N_{cr,Gav}$ (Timoshenko and Gere 1961). The latter critical load can be expressed by Eq. 2, in which GA_v is the shear stiffness of the member.

$$N_{cr} = \frac{\pi^2 EI}{L^2} \tag{1}$$

$$N_{cr,GA_v} = \frac{P_{cr}}{1 + \dfrac{N_{cr}}{GA_v}} \tag{2}$$

Timoshenko and Gere (1961) derived an expression for the critical buckling load of several built-up column types, of which the geometry of columns with batten plates (Fig. 2) matches the cellular and castellated member geometries the best. The battens would correspond with the web posts between the web openings, whereas the longitudinal channels sections could correspond with the tee sections in cellular and castellated members (Fig. 3).
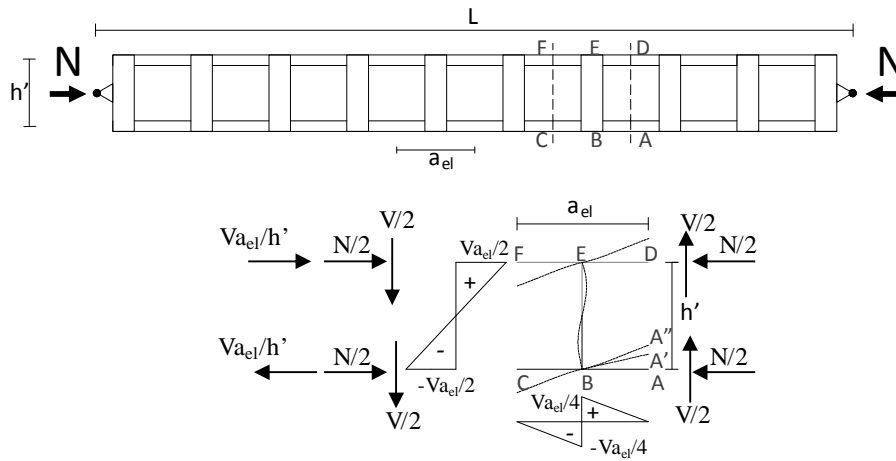

Figure 2: Flexural buckling of battened columns: additional deformation due to local bending moments.

From this battened column, an element FEDCBA is extracted, subjected to a global normal force N, bending moment M and shear force V. These stress resultant are distributed over FEDABC as shown in Fig. 2, assuming that the points of inflection of the deflection curves are situated in the middle of the batten (point H) and in the channels at mid-distance between two battens (points F, D, A and C), just as for a Vierendeel beam. Thus, the local bending moments caused by the shear force are zero at the aforementioned locations. For each element, the additional deflection due to the local bending of the battens and the channels can be calculated. The resulting inverse shear

3

stiffness $1/Ga_v$ of the battened column can be calculated by dividing the angular shear displacement γ by the shear force V (Eq. 3). In this expression, the first term originates from the rotation of the batten in B due to the local bending moment in the battens, with a_{el} the distance between the centers of two adjoining battens, h' the height between the centerlines of the top and bottom section and EI_k the bending stiffness of the battens. The second term originates from the additional bending deflection A'A'' of the channel section, EI_f being the bending stiffness of the top and bottom sections.

$$\frac{1}{GA_v} = \frac{\gamma}{V} = \frac{a_{el}}{12}\left(\frac{h'}{EI_k} + \frac{a_{el}}{2EI_f}\right) \tag{3}$$

In this calculation the local shear deformations, as well as additional deformations of the channel sections due to second order effects are neglected.
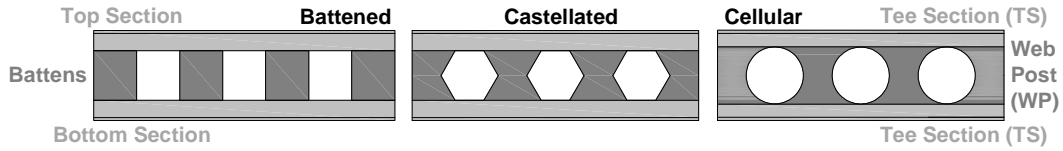

Figure 3: Equivalence of cellular and castellated columns with battened columns.

The approach used for a built-up columns with batten plates could be adapted to take into account local bending deformations around the openings of cellular or castellated columns. This will be further developed in Section 3.

2.2 Approach by (Yuan et al. 2014) for castellated columns
In (Yuan et al. 2014), a derivation of the critical load $N_{cr,Yuan}$ of castellated columns is presented, applying the Ritz method to express the stationarity of the potential energy. Bernoulli's hypothesis is valid for the two tee sections: the rotation of the tee sections is equal to the slope of the deflected member axis. However, this will not be the case for the web post, which will undergo shear deformation. This shear deformation is implemented by assuming an independent axial displacement of the top and bottom tee section. In the derivation, a shear factor $k_{sh}=0.25$ was derived specifically for the common castellated member geometry with regular hexagonal openings and for a Poisson's coefficient ν of 1/3. The shear factor k_{sh} covers both the shear and bending deformation of the web post, considering a rectangular web post with average width.

The critical buckling load $N_{cr,Yuan}$ can be expressed using Eq. 4, using the dimensions from Fig. 4. In this equation, EI_{tee}, is the bending stiffness of one tee about its principal y-axis, A_{tee} the surface of the tee and e the distance between the center of gravity of the complete cross-section and the center of gravity of a tee. This expression for $N_{cr,Yuan}$ was checked numerically for a relatively limited group of 56 castellated column geometries and its suitability will be further examined in Section 5.

$$N_{cr,Yuan} = \frac{2\pi^2 EI_{tee}}{L^2} + \frac{2\pi^2 EA_{tee}e^2}{L^2} \cdot \frac{1}{1+\dfrac{\pi^2 EA_{tee}a}{2k_{sh}t_w GL^2}} \tag{4}$$
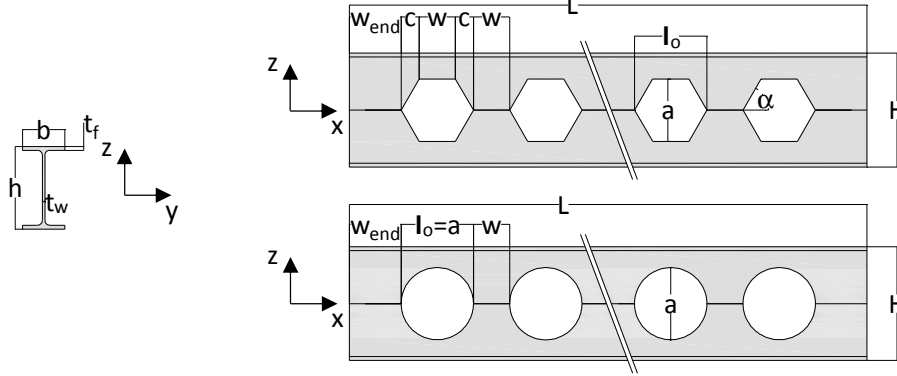
4

Figure 4: Dimensions and coordinate system for cellular and castellated columns.

2.3 Approach by (Gu and Cheng 2016) for cellular columns

Very recently, Gu and Cheng (2016) proposed a formulation for the critical buckling load of cellular columns. Its derivation is very similar to the derivation in (Yuan 2014) for castellated columns, although it is somewhat less detailed. Furthermore, in this derivation the bending deformations of the web were not considered. Following the notations of Fig. 4, the critical buckling load $N_{cr,Gu}$ can be expressed by Eq. 5, with the shear factor k_{sh} given by Eq. 6.

$$N_{cr,Gu} = \frac{2\pi^2 EI_{tee}}{L^2} + \frac{2\pi^2 EA_{tee}e^2}{L^2} \cdot \frac{1}{1 + \frac{\pi^2 EA_{tee}(w+a)}{2k_{sh}L^2}} \tag{5}$$

$$k_{sh} = \frac{Gt_w}{\frac{2a+2w}{\sqrt{w \cdot (w+2a)}} \cdot \arctan\left(\sqrt{\frac{w+2a}{w}}\right) - \frac{\pi}{2}} \tag{6}$$

The validation of the proposed $N_{cr,Gu}$ was very limited, as the results were only compared with numerical results for 13 different cellular column geometries. The suitability of the proposed expression will be further discussed in Section 5.

2.4 Other solutions

Apart from the three approaches mentioned above, it might be useful to compare the obtained numerical values of the critical strong-axis flexural buckling load with the critical buckling load $N_{cr,0}$, using the bending stiffness EI_0 of the gross cross-section at the web post (Eq 7). The reduced bending stiffness of the member could be taken into account by considering the value of the 2T critical buckling load $N_{cr,2T}$ given by Eq. 8. In the latter equation, bending stiffness EI about the strong axis is calculated for the cross-section at the center of the opening. This 2T approach, in which all cross-sectional properties are calculated at the cross-section at the center of the web opening is currently already being used in European pre-standards (CEN 1998) for lateral-torsional buckling, and has been found to be a valid approach for other global buckling modes of castellated and cellular members (Sonck 2014) (Sonck et al. 2012).

5

$$N_{cr,0} = \frac{\pi^2 EI_0}{L^2} \tag{7}$$

$$N_{cr,2T} = \frac{\pi^2 EI_{2T}}{L^2} \tag{8}$$

3. Formulation of expression for critical load

In Section 2.1, the method used to derive the critical moment of battened columns was introduced as a possible approach to calculate the shear stiffness of the perforated web. In its original shape, preliminary investigations showed this approach to be very conservative: it resulted in an overly low shear stiffness. This is caused by the fact that all material is assumed to be located on the center lines of the tee sections and web posts, neglecting the stiffer regions above and below the web post, where the center lines of the tee sections and the web posts intersect. Thus, a modification of the approach for battened columns was proposed, taking into account that part of the web post lines and tee section lines will be rigid. Additionally, equivalent opening dimensions were proposed to be used for the web post width and tee section height. Lastly, the effect of the openings on the overall bending stiffness of the castellated and cellular column was taken into account by using a weighted average.

These adaptations will be further explained in the following sections. It will be assumed that the circular and rectangular openings can be replaced by equivalent rectangular openings with a specific set of dimensions, depending on the considered deformation. However, the distribution of stress resultants, as depicted in Fig. 5, will remain the same. In this figure, h' is the distance between the centers of gravity of the tee sections at the center of the web opening, w the web post width and ℓ_o the opening length.
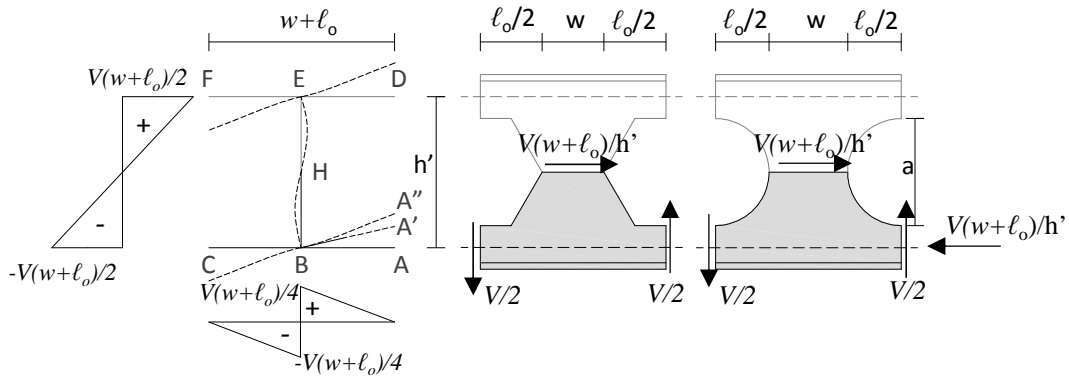

Figure 5. Considered distribution of forces.

3.1 Effect of web post bending

The rotation of the web post ends relative to the chord EB connecting the two web post ends (γ_1 in Fig. 3) can be found using the unit force method on the simply supported member EB (Fig. 6). In the original derivation, the bending stiffness of the web post was constant along EB. However, for the castellated and cellular members, it is assumed that the intersection between the web post and tee section, highlighted in Fig. 6 will not deform ($EI_{WP}=\infty$), resulting in the integral only being non-zero in the central part of the web post. The resulting rotation is given by Eq. 9. In this

expression, EI^*_{WP} is the bending stiffness of the equivalent web post with width w*. This equivalent web post width w* can be calculated by Eq. 10, using Eq. 11 for cellular columns, and Eq. 12 for castellated columns (Fig. 6).

$$\gamma_1 = \int_{BE} \frac{M}{EI_{WP}} m \cdot dx = \frac{Va^3(\ell_o + w)}{12h'^2 EI^*_{WP}} \tag{9}$$

$$w^* = \ell_o + w - \ell^*_o \tag{10}$$

$$\ell^*_{o,cell} = \beta\ell_o = \beta a \tag{11}$$
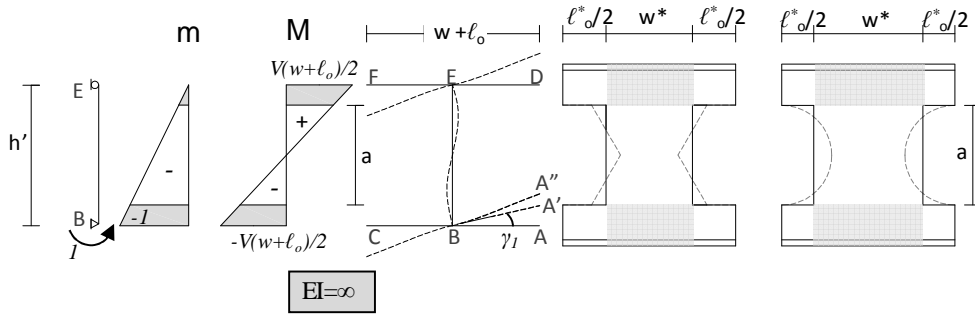
$$\ell^*_{o,cast} = w + \beta \cdot 2c \tag{12}$$

Figure 6: Determination of displacement AA'=$\gamma_1(w+\ell_o)/2$ due to web post bending.
Equivalent web post width w* and opening length ℓ^*_o.

3.2 Effect of tee section bending

The additional deformation A'A'' of the tee section in location A, relative to the tangent in B can again be found using the unit force method on a cantilever beam BA (Fig. 7). In the original expression, the bending stiffness of the beam BA was assumed to be constant. However, for the castellated and cellular members, it is assumed that the intersection between the web post and tee section, highlighted in Fig. 7 will not deform ($EI_{TS}=\infty$), resulting in the integral only being non-zero in the right part of the beam BA with length $\ell_o/2$. The resulting displacement A'A'' is given in Eq. 13. In this expression, the bending stiffness of the equivalent tee section EI^*_{TS} is calculated using an equivalent opening height a* given by Eq. 14 for cellular columns and Eq. 15 for castellated columns (Fig. 9).

$$A'A'' = \int_{BA} \frac{M}{EI_{TS}} m \cdot dx = \frac{V\ell^3_o}{48EI^*_{TS}} \tag{13}$$

$$a^*_{cell} = \alpha a \tag{14}$$

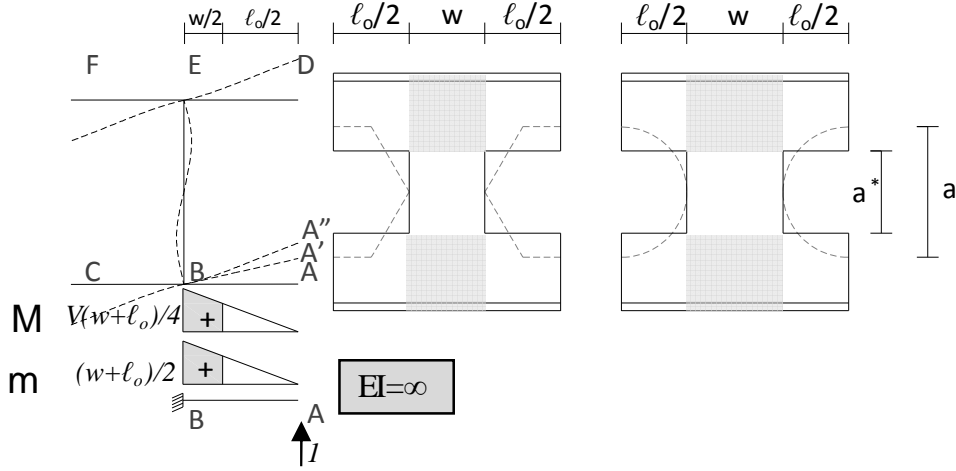$$a^*_{cast} = a\frac{(w + \alpha \cdot 2c)}{w + 2c} \tag{15}$$

Figure 7: Determination of relative displacement A'A" due to tee section bending. Equivalent opening height a*.

3.3 Effect of overall bending

For the larger lengths, the effect of the shear deformation decreases and the effect of the overall bending stiffness EI dominates. It was found that the deviations for these larger lengths were minimal if a weighted average EI^* was used for the overall bending stiffness. The weighted average, given by Eq. 16, was determined by considering the smallest encompassing rectangle for each opening, i.e. the rectangle with height a and length ℓ_o.

$$EI^* = \left(\frac{n \cdot \ell_o}{L} \right) EI_{2T} + \left(1 - \frac{n \cdot \ell_o}{L} \right) EI_0 \tag{16}$$

3.4 Overall expression for GA_v and $N_{cr,Gav}$

Finally, the inverse shear stiffness $1/GA_v$ can be determined by Eq. 17. Using this expression in Eq. 18, the critical load $N_{cr,Gav}$ can be calculated as a function of α and β. In Section 5, these values will vary between 0.45 and 1.00 in steps of 0.05, and the best-fitting values of α and β will be determined.

$$\frac{1}{GA_v} = \frac{\gamma}{V} = \frac{\left[\gamma_1 \left(\frac{\ell_o + w}{2} \right) + A'A'' \right]}{\left(\frac{\ell_o + w}{2} \right) \cdot V} = \frac{a^3(\ell_o + w)}{12h'^2 EI^*_{WP}} + \frac{\ell_o^3}{24(\ell_o + w) EI^*_{TS}} \tag{17}$$

$$N_{cr,GA_v} = \frac{\pi^2 EI^*}{L^2 + \dfrac{\pi^2 EI^*}{GA_v}} \tag{18}$$

4. Numerical model and parametric study

In this section, the numerical model used for the parametric study, as well as the considered parameters during this study are described. The dimensions and the used coordinate system are depicted in Fig. 4.

4.1 Numerical model

The numerical model used for the parametric study was constructed in Abaqus (Dassault Systèmes 2014). The member was modelled using quadratic shell elements with reduced integration (S8R) for the flanges and the web, disregarding the fillet between the flanges and the web.

At both ends, the members were simply supported, preventing all lateral displacements (in y- and z-direction) and rotations about the longitudinal x-axis. At one end, the axial displacement of the central web node was prevented. To prevent weak-axis buckling, additional lateral restraints (in y-direction) were introduced along axial lines at the web to flange intersections, as well as at the centre of the web. Kinematic coupling constraints prevented local deformations of the web at the column ends. The compressive force N was introduced at both ends of the columns as line loads (shell edge loads) on the flanges and the web, of which the sizes would correspond with a uniform compressive stress over the cross-section.

The critical buckling load was determined using a linear buckling analysis. The considered members were all perfectly straight and displayed perfect linear elastic behaviour with the modulus of elasticity E=210 GPa and Poisson's coefficient v=0.3. Using these values, the shear modulus G=E/2/(1+v) can be determined.

4.2 Parametric study

The different critical buckling load formulations from Sections 2 and 3 were checked using the results of a parametric study in which the critical buckling load of a large number of castellated and cellular columns was determined. All considered geometries were fabricated starting from the six hot-rolled I-sections listed in Table 1. It was assumed that these parent sections were cut into two halves according to a certain pattern, after which both halves were shifted and welded together (Fig. 8). The final height H of the castellated or cellular member can be found using Eqs. 19 and 20, assuming a cut width r_b of 8 mm.

Table 1: Considered parent sections and their dimensions.

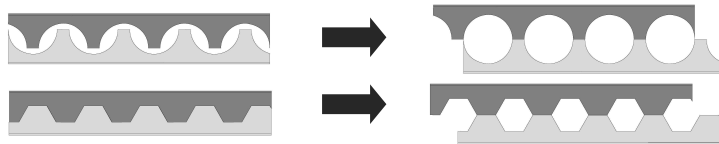|	Total height h (m)	Flange width b (m)	Flange thickness t_f (m)	Web thickness t_w (m)
IPE300	0.300	0.150	0.0107	0.0071
IPE600	0.600	0.220	0.0190	0.0120
HEA320	0.310	0.300	0.0155	0.0090
HEA650	0.640	0.300	0.0260	0.0135
HEM320	0.359	0.309	0.0400	0.0210
HEM650	0.668	0.305	0.0400	0.0210

Figure 8: Fabrication of cellular and castellated members.

$$H = h + \frac{\sqrt{\left(a - 2r_b\right)^2 - w^2}}{2}$$

(19)

$$H = h + \frac{a}{2} = f_H h$$

(20)

The two varying factors for cellular member geometries were the diameter of the opening $a=f_a.h$ and the distance $w=f_w\ell_o=f_w a$ between two openings. By varying the geometry factors f_a and f_w (Table 2) and taking into account the geometric constraints from (CTICM 2006) and (CEN 1998), all realistic cellular geometries made from the selected parent section were considered.

For the castellated geometries, the height of the opening a, the width of the web post $w= f_w\ell_o$ and the opening angle α can vary. The values of the factors f_H and f_w, as well as the opening angle α were varied as mentioned in Table 3. Considering the abovementioned geometric restrictions, a large group of castellated member geometries was considered, going from very narrow openings through regular hexagonal openings to very wide, almost Angelina® like openings.

Table 2: Varied geometry parameters for cellular columns.

f_a	0.8	1.0	1.2
f_w	0.1	0.4	0.7

Table 3: Varied geometry parameters for castellated columns.

f_H	1.4	1.5	1.6
f_w	0.1	0.3	0.5
α	45°	60°	75°

For each considered geometry, five different lengths were considered, so that the corresponding slenderness $\bar{\lambda} = \sqrt{f_y A_{2T} / N_{cr,2T}}$ would be approximately equal to 0.5, 1.0, 1.5, 2 or 2.5. This slenderness was determined using the surface A_{2T} of the cross-section at the center of the opening, a yield stress f_y of 235 MPa and the critical buckling load $N_{cr,2T}$.

In total, 725 different linear buckling analyses were executed: 215 for the cellular columns and 510 for the castellated columns. The lowest eigenvalue obtained for each of these is considered as $N_{cr,abq}$.

5. Results and discussion

In this section, the numerically obtained values of the critical load $N_{cr,abq}$ will be compared with the different critical load formulations for cellular and castellated columns. For each examined geometry and each formulation of N_{cr}, the error Δ can be determined using Eq. 21. If Δ is positive, the formulation is safe (but conservative), while negative Δ values correspond with unsafe formulations.

$$\Delta = \left(\frac{N_{cr,abq}}{N_{cr}} - 1 \right) \cdot 100\%$$

(21)

All considered 725 geometries, with the exception of three castellated columns, failed by flexural buckling about the strong axis. The three deviating buckling modes all occurred for an IPE600 parent section with $f_H=1.4$. They all failed by local buckling of the tee sections at the ends of the column. These three local failure modes will be not further considered in the remainder of this paper.

10

5.1 Existing proposals

In Fig. 9, the numerical results are compared with the most simple expression of all possible formulations: the gross critical buckling load $N_{cr,0}$ (Eq. 7), considering the bending stiffness of the gross-cross section and neglecting shear deformations. As expected, this formulation is unsafe. For the intermediate and longer lengths, this unsafety is relatively small (smaller than 15%), but for the shorter lengths large unsafe errors could be perceived for both the castellated and cellular columns. The latter is due to the effect of the finite shear stiffness of the cross-sections, which becomes increasingly important for shorter lengths. This effect seems to be more severe for the cellular columns. In Tables 4 and 5, numerical values of the minimum and maximum error, as well as its mean value and standard deviation are listed for respectively cellular and castellated columns. This comparison also illustrates the detrimental effect of the web openings on the critical buckling load: the critical buckling load $N_{cr,abq}$ of castellated and cellular columns can be about 30 to 40% smaller than the buckling load obtained for similar columns without web openings.

Another simple approach would be to use $N_{cr,2T}$, as given by Eq. 8 (Fig. 10). Here the effect of the finite shear stiffness is also neglected, but the bending stiffness is calculated for the cross-section at the center of the web opening. As expected, this improves the safety for the longer columns, which now display slight conservative behavior. However, for the shorter lengths, this formulation remain very unsafe. Thus, as already stated by other authors, the shear flexibility of the columns needs to be taken into account to come up with an accurate formulation of the buckling load.
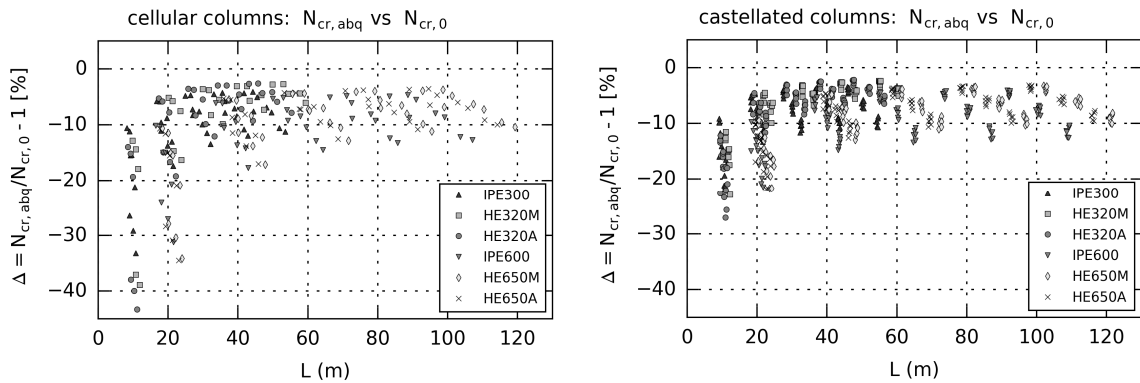

Figure 9: Error Δ between $N_{cr,abq}$ and $N_{cr,0}$ for all considered cellular and castellated columns.
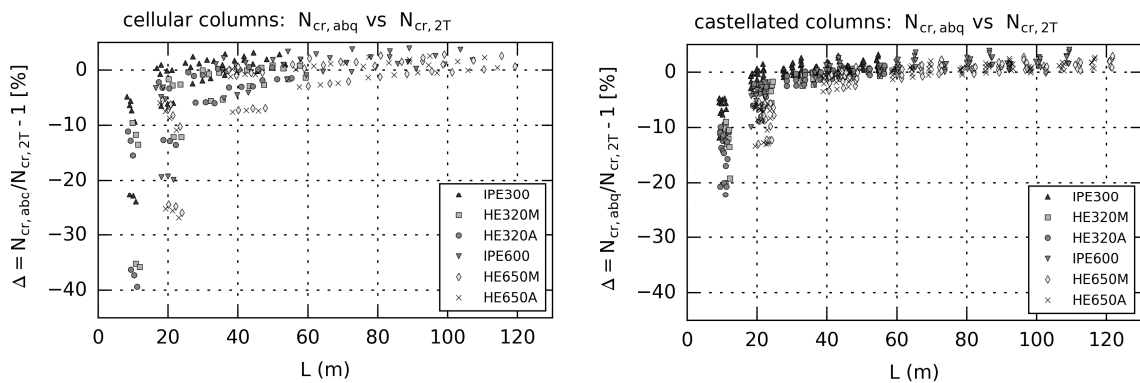

Figure 10: Error Δ between $N_{cr,abq}$ and $N_{cr,2T}$ for all considered cellular and castellated columns.

11

In Figure 11, a comparison is made between the numerical values and the formulations proposed in literature for cellular and castellated columns. It can be seen that the largest unsafe errors are 7% smaller than for $N_{cr,2T}$, which is definitely an improvement (Tables 4 and 5). However, these results are not as good as expected. While the underlying methodology was definitely satisfactory, these formulations could be further improved by considering other trial functions for the buckled shape, taking into account local bending deformations of the tee section and the web post. These unsafe deviations were not noticeable in the original papers due to the limited amount of geometries for which they were validated.
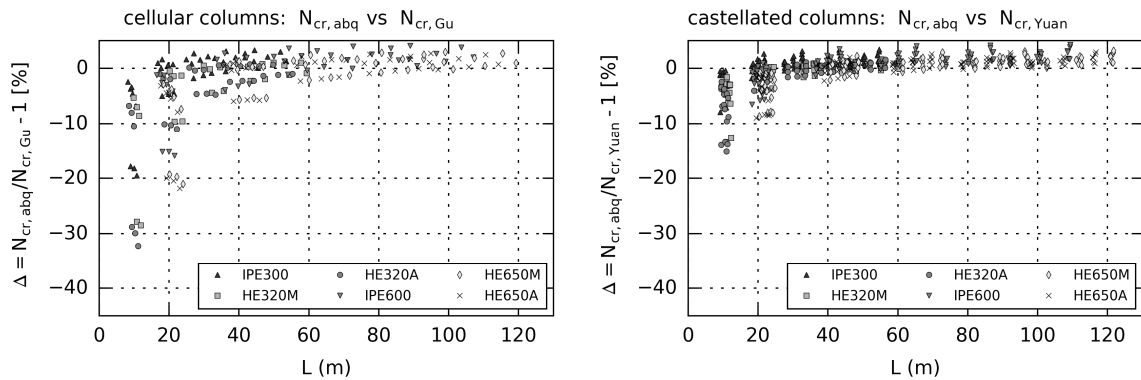

Figure 11: Error Δ between $N_{cr,abq}$ and $N_{cr,Yuan}$ or $N_{cr,Gu}$ for all considered cellular and castellated columns.

5.2 New proposed rule ($N_{cr,Gav}$)

Taking into account the large deviations for the three formulations of N_{cr} considered in the previous section, it will now be investigated whether an important amelioration in the results can be obtained using the new formulation for $N_{cr,Gav}$, which is largely based on the approach used to account for the effect of shear deformation on the critical buckling load of battened columns. As already explained in Section 3, this rule was modified to take into account that the intersections between the schematized web posts and tee sections have finite dimensions and will behave much stiffer. Additional modifications were made by determining the bending stiffness of the web post (EI_{WP}) and the tee section (EI_{TS}) using modified opening dimensions, represented by a factor α for the opening height a^* (in EI_{TS}) and a factor β for the opening length ℓ_o^* (in EI_{WP}). These factors were chosen so that a unity value for both would correspond with calculating EI_{WP} and EI_{TS} using the maximum opening dimensions (the encompassing rectangular opening with length ℓ_o and height a). It was expected that assuming $\alpha=\beta=1.0$ would be too conservative, and this is confirmed by Fig. 12 and the results in Tables 4 and 5: for the shorter lengths this formulation can lead to results that are 6.5 to 8 times too big. Thus, the necessity of using factors α and β smaller than one (and larger than zero) is confirmed.

The results from the parametric study were compared with $N_{cr,Gav}$ using factors α and β which could independently vary between 0.45 and 1.0, with intermediate steps of 0.05. Thus, the best fitting α and β factors could be determined. For all considered values, the overall minimum error Δ_{min}, maximum error Δ_{max}, mean error Δ_{mean}, and standard deviation of the error Δ_{stdev} could be determined. These values are depicted in Fig. 13 for cellular columns and in Fig. 14 for castellated columns. Not all considered α and β values are visible in these figures, as some values caused too large deviations to be visible in the Figures (and to be of practical use). It should be

pointed out that the equivalent openings dimensions are not formulated in a similar manner for cellular and castellated columns (cf. Sections 3.1 and 3.2), which explains their different behavior for similar values of α and β.

Table 4: Minimum Δmin, maximum Δmax, mean Δmean and standard deviation Δstdev for error Δ (all cellular columns). The row with the selected values of α and β is highlighted in grey.

| | β | α | Δ_{min} | Δ_{max} | Δ_{mean} | Δ_{stdev} |
	[-]	[-]	[%]	[%]	[%]	[%]
$N_{cr,0}$	-	-	-43.3	-2.6	-10.8	7.8
$N_{cr,2T}$	-	-	-39.4	4.0	-3.7	8.2
$N_{cr,Gu}$	-	-	-32.2	4.0	-2.4	6.6
$N_{cr,Gav}$	1.00	1.00	-1.1	558.7	55.3	116.3
$N_{cr,Gav}$	0.80	0.85	-11.9	1.1	-1.7	2.2
$N_{cr,Gav}$	0.80	0.90	-11.4	2.2	-1.2	1.9
$N_{cr,Gav}$	0.80	0.95	-10.7	9.0	-0.5	2.2
$N_{cr,Gav}$	0.85	0.80	-6.6	4.9	-0.4	1.9
$N_{cr,Gav}$	0.85	0.85	-5.8	6.2	-0.0	1.9
$N_{cr,Gav}$	0.85	0.90	-4.8	10.4	0.4	2.1

Table 5: Minimum Δ_{min}, maximum Δ_{max}, mean Δ_{mean} and standard deviation Δ_{stdev} for error Δ (all castellated columns). The row with the selected values of α and β is highlighted in grey.

| | β | α | Δ_{min} | Δ_{max} | Δ_{mean} | Δ_{stdev} |
	[-]	[-]	[%]	[%]	[%]	[%]
$N_{cr,0}$	-	-	-27.1	-2.2	-8.5	4.7
$N_{cr,2T}$	-	-	-22.2	4.1	-1.7	4.4
$N_{cr,Gu}$	-	-	-15.2	4.2	-0.2	2.8
$N_{cr,Gav}$	1.00	1.00	-2.9	709.6	33.7	91.0
$N_{cr,Gav}$	0.45	0.7	-10.5	2.8	-1.2	1.8
$N_{cr,Gav}$	0.45	0.75	-8.4	2.9	-1.1	1.8
$N_{cr,Gav}$	0.45	0.8	-7.1	6.3	-0.8	1.8
$N_{cr,Gav}$	0.5	0.7	-10.3	2.8	-1.0	1.7
$N_{cr,Gav}$	0.5	0.75	-8.2	3.3	-0.9	1.7
$N_{cr,Gav}$	0.5	0.8	-6.3	6.5	-0.6	1.8
$N_{cr,Gav}$	0.55	0.7	-10.1	4.4	-0.8	1.8
$N_{cr,Gav}$	0.55	0.75	-8	4.5	-0.6	1.8
$N_{cr,Gav}$	0.55	0.8	-5.5	6.8	-0.4	1.8
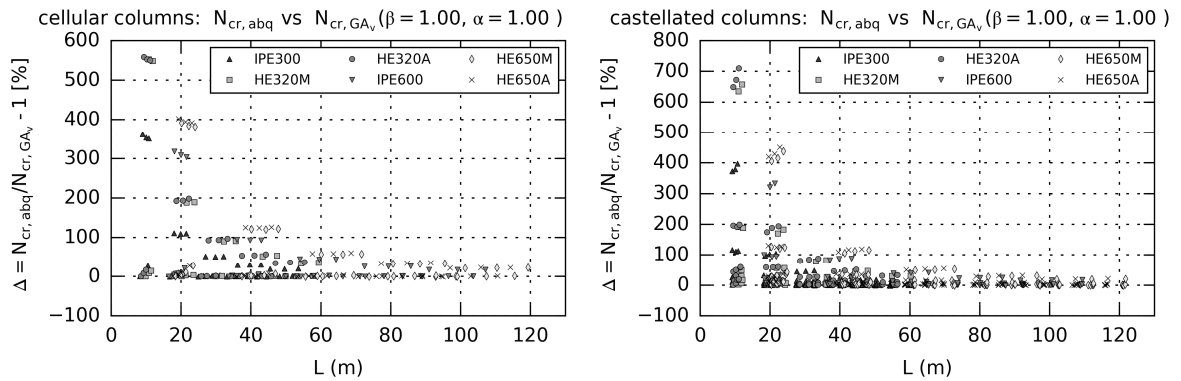
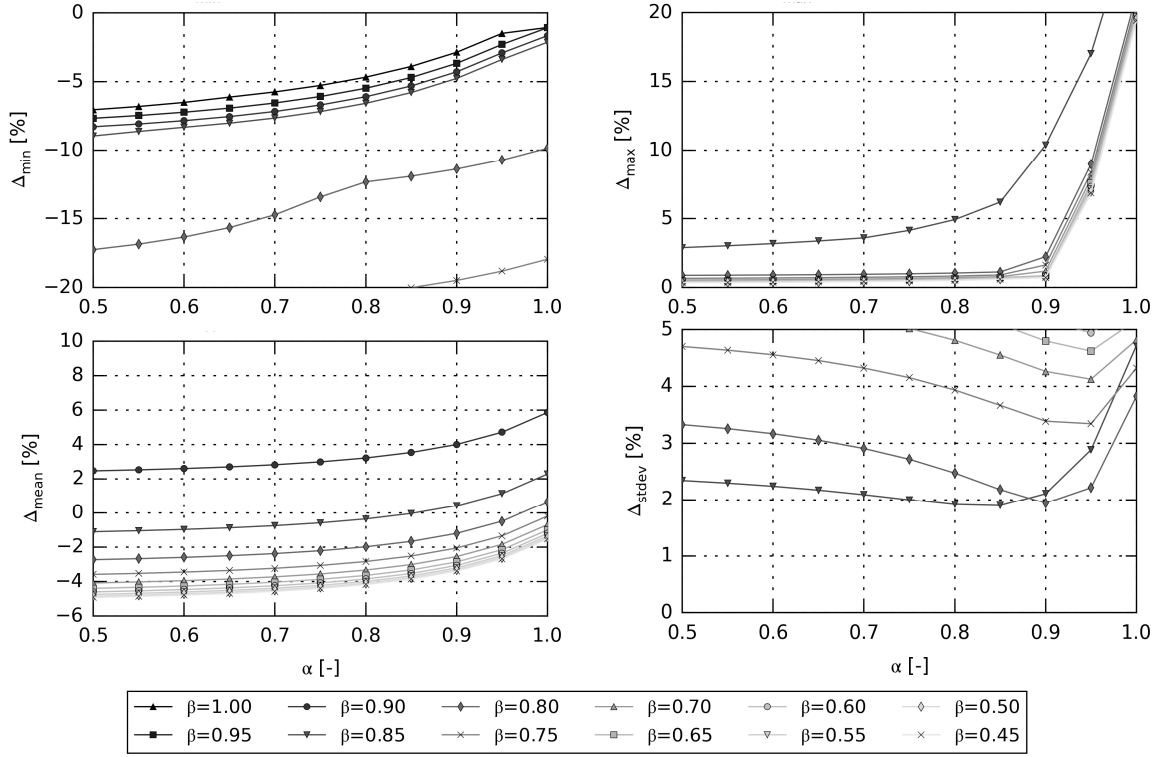Figure 12: Error Δ between $N_{cr,abq}$ and $N_{cr,Gav}$ for all considered cellular and castellated columns (α=β=1).

Figure 13: Minimum Δ_{min}, maximum Δ_{max}, mean Δ_{mean} and standard deviation Δ_{stdev} for error Δ between $N_{cr,abq}$ and $N_{cr,Gav}$ (cellular columns).

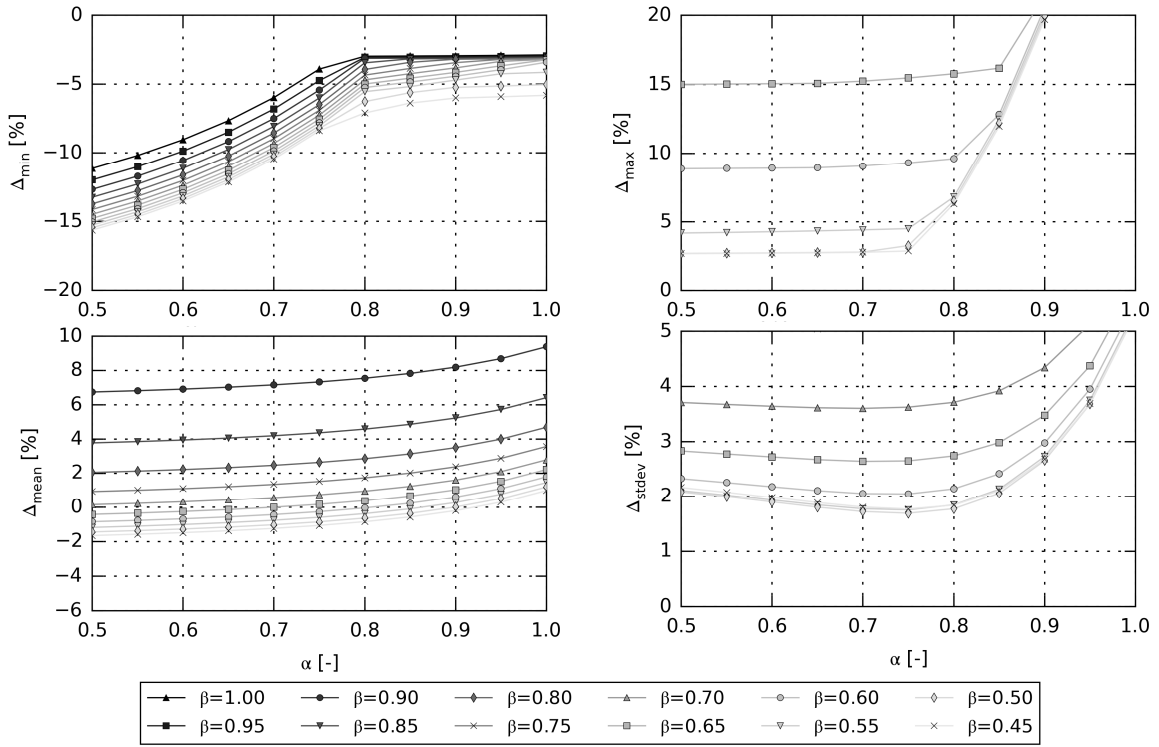Figure 14: Minimum Δ_{min}, maximum Δ_{max}, mean Δ_{mean} and standard deviation Δ_{stdev} for error Δ between $N_{cr,abq}$ and $N_{cr,Gav}$ (castellated columns).

Overall, Figs. 13 and 14 illustrate that Δ_{min}, Δ_{max} and Δ_{mean} increase with increasing values of α and β. This is expected, as the formulation grows more conservative with increasing equivalent opening sizes. However, the standard deviation of the error Δ_{stdev} display a clear minimum. For cellular columns, this minimum corresponds with values of β of 0.8 and 0.85, while α is about 0.8. For the castellated columns, this minimum corresponds with values of β of 0.45, 0.5 or 0.55, while α is about 0.75. Detailed values of Δ_{min}, Δ_{max}, Δ_{mean} and Δ_{stdev} for these α and β values are listed in Tables 4 and 5. These errors are certainly more acceptable than those obtained for all earlier considered N_{cr} formulations. Although the results for some combinations of α and β lie very closely together, the selection for the optimal α and β factors was made by aiming for equal magnitudes of the maximum and minimum error. For cellular members it is proposed to use $\alpha=\beta=0.85$, and for the castellated members it is proposed to use $\alpha=0.8$ and $\beta=0.5$. The obtained errors Δ obtained for the selected α and β factors are depicted in Fig. 15 for all considered columns. Compared with the other considered (existing) formulations, the match with the numerical results has been considerably improved.

In the proposed formulation, a weighted average approach was used for the overall strong-axis bending stiffness of the column (cf. section 3.3). The good fit of this approach is visible for the intermediate and longer lengths in Fig. 15, for which the effect of the shear flexibility is less substantial.
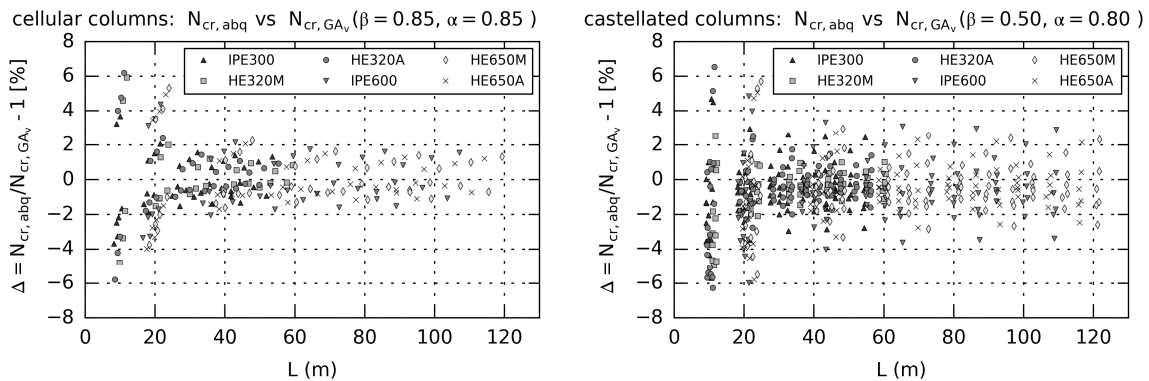

Figure 15: Error Δ between $N_{cr,abq}$ and $N_{cr,Gav}$ for all considered cellular and castellated columns ($\alpha=\beta=0.85$ for the cellular columns; $\beta=0.5$ and $\alpha=0.8$ for the castellated columns).

6. Conclusions

In this paper, different formulations for the critical flexural buckling load about the strong axis N_{cr} of cellular and castellated columns were examined numerically. The goal of these formulations was to take into account the effect of the web openings, which mainly increased the shear flexibility of the web, decreasing the critical buckling load. Compared with analytical values obtained for unperforated columns of the same geometry, the numerically obtained values of N_{cr} could be up to 40% smaller.

For both cellular and castellated columns, formulations for N_{cr} that should take into account the shear deformation of the web post were already described in literature. While an extensive numerical check of these proposals demonstrated that the unsafe deviations were somewhat decreased, the decrease was not substantial enough. For small lengths, the obtained formulation was still too unsafe.

15

Based on an adaptation of the existing formulation of N_{cr} for battened columns, the authors formulated an approach that included the local bending deformations around the web openings. By considering different options for the equivalent opening size used to determine the local bending stiffness of the web post and tee sections, a best-fitting equivalent opening size could be determined for the cellular and castellated columns. The deviations following this approach were found to be very acceptable (max. 6.5 % error). The effect of the local shear deformations of the web posts and tee sections is assumed to be implicitly included in the best fitting equivalent opening.

In further research, the formulation for the elastic critical buckling load N_{cr} can be used in a study of the strong-axis buckling resistance N_{Rd}, considering geometric nonlinear behavior, imperfections and plasticity of the steel. While the current paper focused on the effect of the modified geometry of the cellular or castellated columns on buckling behavior, in this future research the imperfections will also be altered. This is due to the modification of the residual stress pattern that takes place during the production process.

References
CEN. (1998). ENV 1993-1-1. "Eurocode 3: Design of steel Structures. Part 1-1: General rules and rules for buildings. Annex N: Openings in webs."

CTICM. (2006). "Arcelor Cellular Beams: Detailed Technical Description."

Dassault Systèmes. (2014). "Abaqus v6.14-1."

Ellobody, E. (2011). "Interaction of buckling modes in castellated steel beams." *Journal of Constructional Steel Research*, 67(5), 814–825. doi:10.1016/j.jcsr.2010.12.012

El-Sawy, K. M., Sweedan, A. M. I., & Martini, M. I. (2009). "Major-axis elastic buckling of axially loaded castellated steel columns." *Thin-Walled Structures*, 47(11), 1295–1304. doi:10.1016/j.tws.2009.03.012

Gu, J., & Cheng, S. (2016). "Shear effect on buckling of cellular columns subjected to axially compressed load." *Thin-Walled Structures*, 98, 416–420. doi:10.1016/j.tws.2015.10.019

Nethercot, D. a., & Kerdal, D. E.-Dd. (1982). "Lateral-torsional buckling of castellated beams." *The Structural Engineer*, 60B(3), 53–61.

Nseir, J., Lo, M., Sonck, D., Somja, H., Vassart, O., & Boissonnade, N. (2012). "Lateral Torsional Buckling of Cellular Steel Beams." *Proceedings of the Annual Stability Conference Structural Stability Research Council (SSRC2012)*. Grapevine, Texas.

Sonck, D., Boissonnade, N., & Van Impe, R. (2012). "Instabilities of cellular members loaded in bending or compression." *Proceedings of the Annual Stability Conference Structural Stability Research Council (SSRC2012)*. Grapevine, Texas.

Sonck, D. (2014). *Global Buckling of Castellated and Cellular Steel Beams and Columns.* PhD dissertation. Ghent University. http://hdl.handle.net/1854/LU-4256332

Sonck, D., & Belis, J. (2015). "Lateral–torsional buckling resistance of cellular beams." *Journal of Constructional Steel Research*, 105, 119–128. doi:10.1016/j.jcsr.2014.11.003

Sweedan, A. M. I., El-Sawy, K. M., & Martini, M. I. (2009). "Identification of the buckling capacity of axially loaded cellular columns." *Thin-Walled Structures*, 47(4), 442–454. doi:10.1016/j.tws.2008.08.009

Timoshenko, S. P., & Gere, J. M. (1961). *"Theory of elastic stability"* (2nd ed.). McGraw-Hill Book Company.

Yuan, W., Kim, B., & Li, L. (2014). "Buckling of axially loaded castellated steel columns." *Journal of Constructional Steel Research*, 92, 40–45. doi:10.1016/j.jcsr.2013.10.013

Zirakian, T., & Showkati, H. (2006). "Distortional buckling of castellated beams." *Journal of Constructional Steel Research*, 62(9), 863–871. doi:10.1016/j.jcsr.2006.01.004